NANO LETTERS

2001
Vol. 1, No. 6
295−298

A House of Cards Structure in Polypropylene/Clay Nanocomposites under Elongational Flow

Masami Okamoto,*,† Pham Hoai Nam,† Pralay Maiti,† Tadao Kotaka,† Naoki Hasegawa,‡ and Arimitsu Usuki‡

Advanced Polymeric Materials Engineering, Graduate School of Engineering, Toyota Technological Institute, Hisakata 2-12-1, Tempaku, Nagoya 468-8511, Japan and Toyota Central R&D Laboratories, Inc., Nagakute, Aichi 480-1192, Japan

Received February 22, 2001 *(Revised Manuscript Received May 1, 2001)*

ABSTRACT

This Letter describes the first real space observation for the formation of a house of cards structure in polypropylene/clay nanocomposite melt under elongational flow by TEM analysis. Both strong strain-induced hardening and rheopexy features are originated from the perpendicular alignment of the silicate layers to the stretching direction.

Development of polymer/clay nanocomposites (PCNs) is one of the latest evolutionary step of the polymer technology. The nanocomposites offer attractive potential for diversification and application of conventional polymeric materials.[1−3] To innovate on the material properties of the nanocomposites, we have to understand the material behavior and control the dispersed morphology with nanometer dimensions.

In a series of our recent studies on PCN using lipophilized smectic clay minerals,[4−6] first we attempted to obtain PCN by dispersing clay particles in a vinyl monomer−initiator mixture that was subsequently allowed to polymerize. It turned out in this system that, as the monomers polymerized, the clay particles were flocculated and segregated out of the system. Then we attempted to control the dispersed structure of clay particles by introduction of polar comonomers to the monomer−catalyst mixture to affect the features of aggregation and flocculation through edge−edge interactions of the layered clay particles.[4,6,7]

Recently, dynamic properties of the polyamide-6 nanocomposite with end-tethered polymer chains and nanocomposite based on polyamide-12 under oscillatory shear were first investigated by Giannnelis[8] and Kressler,[9] respectively. However, to our knowledge, there have been no precision studies so far reported on the rheological and structural analyses of the nanocomposite under flow fields, although many studies are available on the dispersed structure under a quiescent state. A main objective of this paper is to investigate the feature of the elongational flow-induced structure formation of nanocomposites. Knowledge of such rheological behavior accompanying the structural formation should be important for assessing the performance of nanocomposites in their processing operation.

The material examined in this study was polypropylene (PP)/clay nanocomposite composed of 0.2 wt % maleic anhydride (MA) modified PP and montmorillonite intercalated with stearylammonium ion via a melt extrusion process, using a twin-screw extruder operated at 200 °C. The MA-modified PP has the weight-average molecular weight $M_w = 19.5 \times 10^4$ and $M_w/M_n = 2.98$, as determined on a gel permeation chromatograph (HLC-8121 GPC/HT Tosoh Co.) with polystyrene elution standards in trichlorobenzene at 140 °C. The melting temperature T_m was 141 °C, as determined on a temperature-modulated differential scanning calorimeter (MDSC, TA Instruments) operated at heating rate of 5 °C/min. Introduction of a minute amount of MA was sufficient to achieve favorable interaction between the PP matrix and dispersed silicate layers.[10]

The PP/clay nanocomposite containing 4 wt % clay (PP/clay(4)) forms a fine dispersion of the silicate layers of about 150 nm length and about 5 nm thickness in the PP matrix (cf. Figure 3) from transmission electron microscopy (TEM) observation.[5] However, on wide-angle X-ray diffraction (XRD) of the same PP/clay(4) we still identified Bragg difraction peaks presumably resulting from a few layers of ordered clay particles remaining in the composite due to the intercalation of PP chains in the silicate galleries.[5] The observed diffraction angle was $2\Theta = 2.97°$ for the (001) plane, leading to the basal spacing of $d_{(001)} \cong 2.79$ nm, which

* Corresponding author. E-mail: okamoto@toyota-ti.ac.jp. Tel: +81-52-809-1861. Fax: +81-52-809-1864.
† Toyota Technological Institute.
‡ Toyota Central R&D Laboratories, Inc.

10.1021/nl0100163 CCC: $20.00
Published on Web 05/22/2001

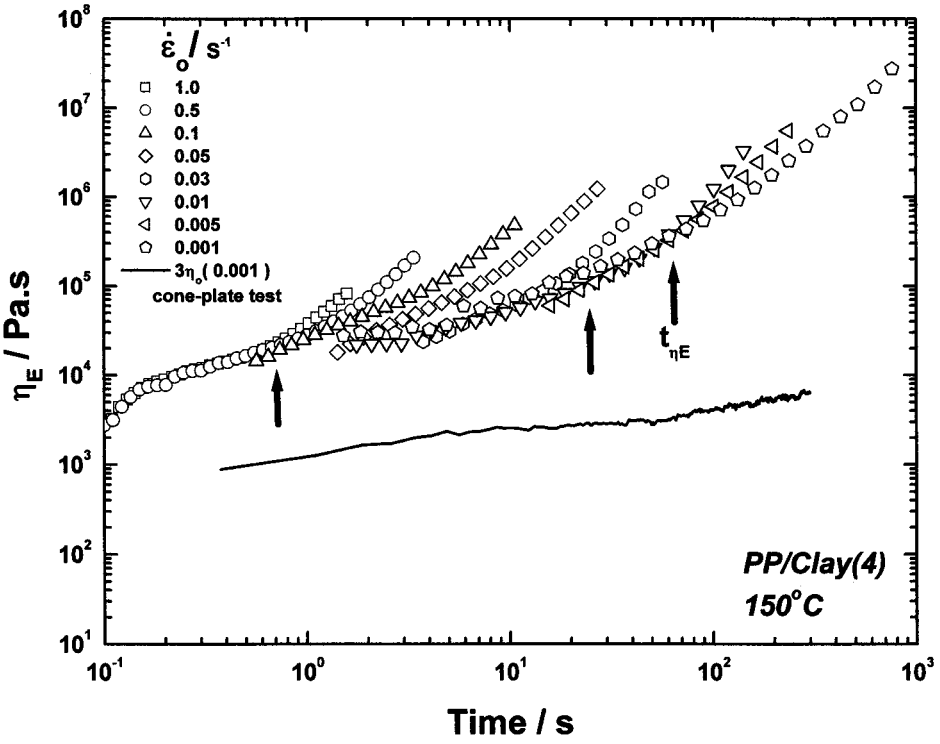

Figure 1. Time variation of elongational viscosity $\eta_E(\dot{\epsilon}_0;t)$ for PP/clay(4) melt at 150 °C. The upward arrows indicate up-rising time t_{η_E} for $\dot{\epsilon}_0 = 1.0$, 0.01, and 0.001 s^{-1} (see text). The solid line shows 3 times the shear viscosity, $3\eta_0(\dot{\gamma};t)$, taken at a low shear rate $\dot{\gamma} = 0.001$ s^{-1} on a cone-plate rheometer.

is about 20% larger than the spacing $d_{(001)} \cong 2.31$ nm (calculated from $2\Theta = 3.81°$) for the lipophilized montmorillonite solid.

An uniaxial elongation test at constant Hencky strain rate $\dot{\epsilon}_0$ in the melt state was conducted on our recently developed elongational flow optorheometry,[11] such as Meissner's new elongational rheometer[12] (commercialized as RME from Rheometric Scientific). The details of the instrumentation are described elsewhere.[11]

On each run of the elongation test, samples of 60 × 7 × 1.0 mm^3 size were annealed at a predetermined temperature (above T_m) for 3 min before starting the run in the rheometer, and uniaxial elongation experiments were carried out at various $\dot{\epsilon}_0$ ranging from 0.001 to 1.0 s^{-1}. The elongated specimens were recovered at various stages of elongation and the developed dispersed structure was observed by TEM (H-7100, Hitachi Co., operated at an acceleration voltage of 100 kV) with a microtomed thin section of about 70 nm without staining.

Figure 1 shows double-logarithmic plots of transient elongational viscosity $\eta_E(\dot{\epsilon}_0;t)$ against time t observed for PP/clay(4) at 150 °C with different Hencky strain rates ϵ_0 ranging from 0.001 to 1.0 s^{-1}. The solid curve represents 3-fold shear viscosity $3\eta_0(\dot{\gamma};t)$, with a constant shear rate of $\dot{\gamma} = 0.001$ s^{-1} at 150 °C. We see in Figure 1 a strong tendency of *strain-induced hardening*[11] for the PP/clay(4) melt. In the early stage, $\eta_E(\dot{\epsilon}_0;t)$ gradually increases with t but independent of $\dot{\epsilon}_0$, which we call the *linear* region of the $\eta_E(\dot{\epsilon}_0;t)$ curve. After a certain time t_{η_E}, which we call the *up-rising* time (marked with the upward arrows), dependent on $\dot{\epsilon}_0$, we see rapid upward deviation of $\eta_E(\dot{\epsilon}_0;t)$ from the curves of the linear region.

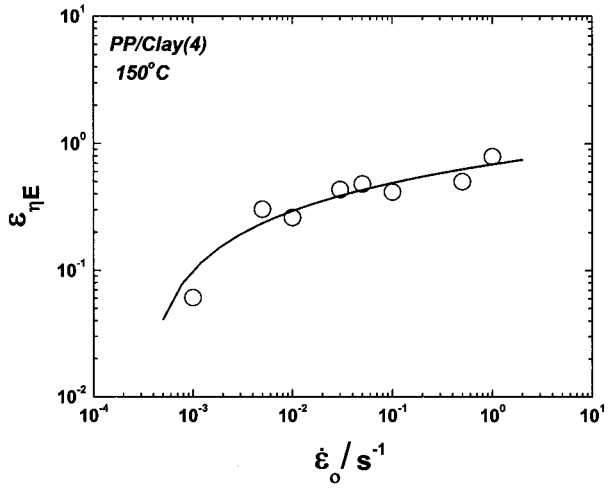

Figure 2. Strain rate $\dot{\epsilon}_0$ dependence of up-rising Hencky strain $\dot{\epsilon}_{\eta_E}$.

On the other hand, we see two features for the shear viscosity curve. First, the extended Trouton rule, $3\eta_0(\dot{\gamma}_0;t) \cong \eta_E(\dot{\epsilon}_0;t)$, does not hold for PP/clay(4) melt, as opposed to the melt of ordinary homopolymers. The latter, $\eta_E(\dot{\epsilon}_0;t)$, is more than 10 times larger than the former, $3\eta_0(\dot{\gamma}_0;t)$. Second, again unlike ordinary polymer melts, $3\eta_0(\dot{\gamma}_0;t)$ of the PP/clay(4) melt increases continuously with t never showing a tendency of reaching a steady state within the time span (5 min or longer) examined here. This *time-dependent thickening* behavior may be called *rheopexy*. The difference reflects a difference in the shear flow-induced versus elongation-induced internal structures of the nanocomposite melt.

The $\eta_E(\dot{\epsilon}_0;t)$ of the matrix MA-modified PP without clay was so low ($<10^4$ Pa s) that we could not determine the

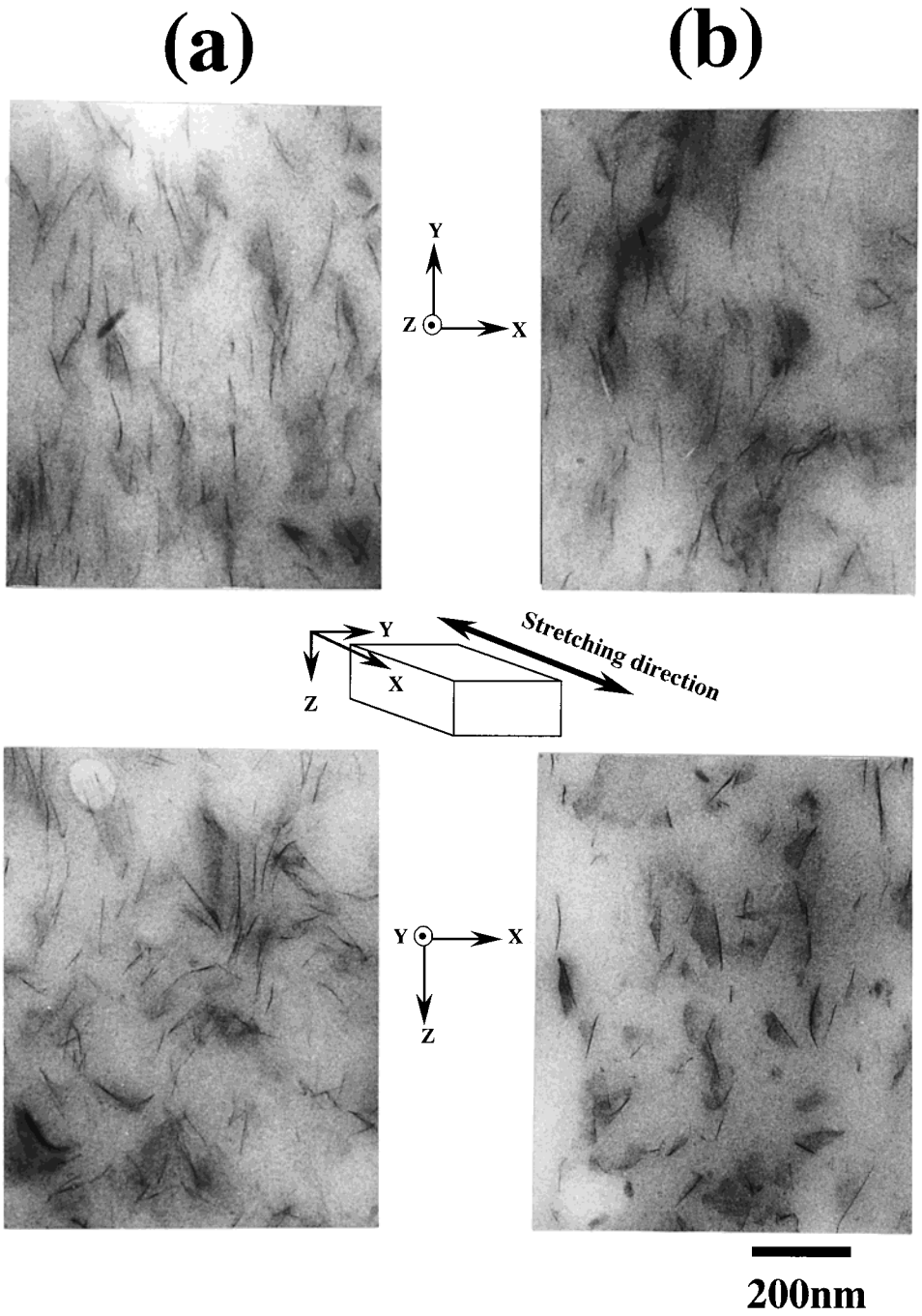

Figure 3. TEM micrographs showing PP/clay(4) elongated at 150 °C with (a) $\dot{\epsilon}_0 = 1.0\ s^{-1}$ up to $\epsilon = 1.3$ ($\lambda = 3.7$) and (b) $\dot{\epsilon}_0 = 0.001\ s^{-1}$ up to $\epsilon = 0.5$ ($\lambda = 1.7$), respectively. Upper pictures are in the $x-y$ plane, and lower ones are in $x-z$ plane along the stretching direction.

accurate value at 150 °C. However, we have confirmed that neither strain-induced hardening in elongation nor rheopexy in shear flow took place in neat PP melt having $M_w = 18.7 \times 10^5$ and $M_w/M_n = 7.50$. These results imply that flow-induced internal structural change occurs in both shear and elongational flow, but the changes are quite different from each other, as judged from the above results on $\eta_E(\dot{\epsilon}_0;t)$ and $3\eta_0(\dot{\gamma}_0;t)$. The rheopexy observed for $3\eta_0(\dot{\gamma}_0;t)$ of PP/clay-(4) at constant $\dot{\gamma}$ reflects a fact that the shear-induced structural change involved a process with an extremely long relaxation time, especially under slow shear field. In our previous study on lipophilized smectic clay/toluene suspensions,[13] we observed similar shear-induced flocculation of the clay particles (in fact, thin plates of a few nanometers thickness) with a time scale of as long as $>10^3$ s in the slow shear field.

As to the elongation-induced structure development, we show in Figure 2 $\dot{\epsilon}_0$ dependence of the up-rising Hencky strain $\epsilon_{\eta_E} = \dot{\epsilon}_0 t_{\eta_E}$ taken for PP/clay(4) at 150 °C. The up-rising Hencky strain ϵ_{η_E} increases with strain rate $\dot{\epsilon}_0$: The lower the $\dot{\epsilon}_0$, the smaller is the value of ϵ_{η_E}. This tendency probably corresponds to the rheopexy of PP/clay(4) under slow shear flow. For a homopolymer, for example, low-density polyethylene (LDPE) melt,[11] strain-induced hardening took place at a common Hencky strain ϵ_{η_E} ($\sim$const) insensitive to either $\dot{\epsilon}_0$ or elongation temperature.[11]

To clarify the complex internal structure formation under elongation, we carried out TEM observation for elongated specimens. The elongated specimens were rapidly quenched by placing it between cold metal plates to freeze the internal structure developed during elongation. Figure 3 shows typical TEM micrographs of the center parts of recovered samples up to (a) Hencky strain $\epsilon = 1.3$ (stretching ratio $\lambda = 3.7$) with $\dot{\epsilon}_0 = 1.0\ s^{-1}$ and (b) $\epsilon = 0.5$ ($\lambda = 1.7$) with $\dot{\epsilon}_0 = 0.001\ s^{-1}$. The *x*- and *y*-axes of the elongated specimen correspond to parallel and perpendicular to the stretching direction. The converging flow is applied to the thickness direction (*y*- and *z*-axis) with stretching, if the assumption of *affine* deformation without volume change is valid. Interestingly, for the specimen elongated with high $\dot{\epsilon}_0$ ($=1.0\ s^{-1}$), we see nicely perpendicular alignment of the silicate layers (edges) along the stretching direction (*x*-axis) in the $x-y$ plane. For the $x-z$ plane, the silicate layers (edges) disperse into the PP matrix along *z*-axis direction rather than randomly, but we cannot see these faces in this plane.

On the other hand, for the low $\dot{\epsilon}_0$ ($=0.001\ s^{-1}$) elongation, the silicate layers (edges) exhibit the perpendicular alignment in the $x-z$ plane, but coherent order of the orientation seemed to be lower than that of rapid stretching case. We see clearly many faces of the dispersed silicate layers in the $x-z$ plane. Of course, there are silicate edges flipped with an inclination of 90° by changing direction along the stretching direction. Here, it should be emphasized that the planar orientation of the silicate faces take place prominently along the $x-z$ plane (unfortunately, we did not observe the images of the $y-z$ plane). According to the two-directional TEM analysis, we can conclude the formation of *a house of cards*-like structure[14] under slow elongation ($\dot{\epsilon}_0 = 0.001\ s^{-1}$). In a similar manner as slow shear flow, the flocculation (relaxation of the structure) might prevail under very slow stretching owing to the long time relaxation. These experimental findings are presumably the first accomplishment of the real space observation for the house of cards structure in a nanocomposite containing layered clays. The house of cards structure is probably a typical example of manifestation of microflocculation through electrostatic attractions between the positively charged edges and the negatively charged faces of the individual silicate layers. This structure leads to gelation of the system, thus imparting elastic gellike properties to the molten nanocomposite. As seen in Figure 1, $\eta_E(\dot{\epsilon}_0;t)$ with $\dot{\epsilon}_0 = 0.001\ s^{-1}$ shows abrupt increasing beyond t_{η_E} by a 3 order higher magnitude. For both stretching cases, both strong strain-induced hardening (cf. Figure 1) and ϵ_{η_E} versus $\dot{\epsilon}_0$ behaviors (cf. Figure 2) must have originated from alignment of the silicate layers perpendicular to but not parallel to the flow direction.

The perpendicular alignment of disklike clay particles with large anisotropy toward the flow direction might sound unlikely, but this could be the case especially under an elongational flow field, in which the extensional flow rate is the square of the converging flow rate along the *y*- and *z*-directions. Obviously, under such conditions, the energy dissipation rate due to viscous resistance between the disk surface and the matrix polymer is minimal, when the disks are aligned perpendicular to the flow direction.

Another possible reason for the formation of the house of cards structure may arise from interactions between silicate layers and the modified PP matrix with a small amount of MA groups,[5,14] which is effective even under the quiescent state. Some 20 years ago van Olphen[14] pointed out that the electrostatic attraction between the layers of natural clay in an aqueous suspension arises from the higher polar force in the medium. The intriguing features such as yield stress thixotropy and/or rheopexy exhibited in aqueous suspensions of natural clay minerals may be taken as a reference to the present polymer/clay nanocomposites.

References

(1) Usuki, A.; Kawasumi, M.; Kojima, Y.; Okada, A.; Kurauchi, T.; Kamigaito, O. *J. Mater. Res.* **1993**, *8*, 1174−1178.
(2) LeBaron, P. C.; Wang, Z.; Pinnavaia, T. J. *Appl. Clay Sci.* **1999**, *15*, 11−29.
(3) Alexandre, M.; Dubois, P. *Mater. Sci. Eng.* **2000**, *28*, 1−63.
(4) Okamoto, M.; Morita, S.; Taguchi, H.; Kim, Y. H.; Kotaka, T.; Tatayama, H. *Polymer* **2000**, *41*, 3887−3890.
(5) Okamoto, M.; Morita, S.; Kim, Y. H.; Kotaka, T.; Tatayama, H. *Polymer* **2001**, *42*, 1201−1206.
(6) Okamoto, M.; Morita, S.; Kotaka, T. *Polymer* **2001**, *42*, 2685−2688.
(7) Okamoto, M.; Taguchi, H.; Sato, H.; Kotaka, T.; Tatayama, H. *Langmuir* **2000**, *16*, 4055−4058.
(8) Krishnamoorti, R.; Giannelis, E. P. *Macromolecules* **1997**, *30*, 4097−4102.
(9) Hoffman, B.; Kressler, J.; Stoppelmann, G.; Friedrich, Chr.; Kim, G. M. *Colloid. Polym. Sci*. **2000**, *278*, 629−636.
(10) Hasegawa, N.; Okamoto, H.; Kato, M.; Usuki, A. *J. Appl. Polym. Sci.* **2000**, *78*, 1918−1922.
(11) Kotaka, T.; Kojima, A.; Okamoto, M. *Rheol. Acta* **1997**, *36*, 646−657.
(12) Meissner, J.; Hostettler, J. *Rheol Acta* **1994**, *33*, 1−21.
(13) Okamoto, M.; Sato, H.; Taguchi, H.; Kotaka, T. *Nihon Reoroji-Gakkaishi* **2000**, *28*, 199−200.
(14) van Olphen, H. *An Introduction to Clay Colloid Chemistry*; Wiley: New York, 1977.

NL0100163